

Long-Term Stabilization/Solidification of Arsenic-Contaminated Sludge by a Blast Furnace Slag-Based Cementitious Material: Functions of CaO and NaCl

Hong Quan, Hui-juan Yu, Xue Yang, Dong-peng Lv, Xing Zhu, and Yuan-cheng Li*



Cite This: *ACS Omega* 2022, 7, 32631–32639



Read Online

ACCESS |



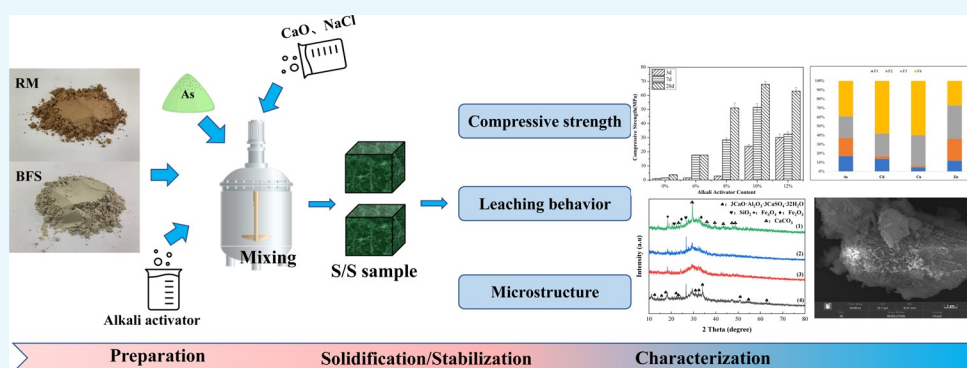
Metrics & More



Article Recommendations



Supporting Information



ABSTRACT: Arsenic is a kind of element widely distributed in the environment that may pose a threat to the ecological environment and human health, while effective remediation and sustainable utilization of arsenic-containing sludge is a challenge. Based on stabilization/solidification blast furnace slag-based cementitious materials (BCMs), this study innovatively proposes to improve the arsenic (As) solidification efficiency and long-term stability by using the activation mode of CaO and NaCl. The effects of different factors on the properties of the BCM were measured by unconfined compressive strength (UCS) tests, X-ray diffraction, Fourier transform infrared spectroscopy, and scanning electron microscopy. The long-term stability and safety of the BCM were verified by leaching toxicity and improved three stage continuous extraction method (BCR) tests. Experimental results show that the addition of CaO provides conditions for the formation of ettringite (AFt), thus promoting the crystal growth of AFt. The addition of NaCl can promote the formation of Cl-AFt and play a good long-term stabilizing role. When the content of the alkali activator is 10% and the modulus is 1.0, the contents of CaO and NaCl are 10 and 1%, respectively. The BCM has the best efficiency in terms of UCS and As solidification. The UCS at 28 days was 5.4 MPa, and the leaching concentration of As was 0.309 mg/L, and the As solidification efficiency was up to 99.9%. In the improved BCR test, the proportions of residual and oxidizable states of arsenic increased by 19.6 and 13.5%, respectively, and the stability of heavy metals improved. These findings show that the BCM has good long-term stability and safety. Overall, this study shows that CaO and NaCl significantly increase the output of AFt and achieve the purpose of efficient and stable solidification of As by the BCM.

1. INTRODUCTION

Arsenic (As) produced in the nonferrous industry forms As-contaminated sludge after treatment, and the content of As in the sludge accounts for approximately 0.23–6.9%. More than 32 million tons of As-contaminated sludge are estimated to be produced from nonferrous metals every year. Given its complex composition, As-contaminated sludge is difficult to treat,^{1–4} causing various environmental problems.^{5,6} Solidification/stabilization is an important method to treat waste containing heavy metals.^{7,8} Previous research and engineering practice have shown that this technology usually uses ordinary Portland cement (OPC) as a binder to solidify waste containing heavy metals. However, OPC production uses a large amount of energy and generates a large volume of

greenhouse gases.^{9,10} In addition, OPC production requires large amounts of nonrenewable raw materials. At present, China is promoting sustainable development and a low-carbon lifestyle and has set the goal of achieving carbon neutrality.¹¹ Therefore, the long-term use of OPC to solidify waste containing heavy metals is inappropriate for this goal. Some scholars pointed out that most metallurgical waste slag

Received: July 8, 2022

Revised: August 17, 2022

Accepted: August 19, 2022

Published: August 29, 2022



Table 1. Chemical Composition of Raw Materials (wt %)^a

ingredient	Na ₂ O	MgO	Al ₂ O ₃	SiO ₂	SO ₃	Cl	CaO	Fe ₂ O ₃
RM	11.34	0.74	37.56	17.71	1.23	0.22	12.79	10.68
BFS	1.06	6.80	12.93	33.19	1.13	ND	38.52	0.598

^aNote: ND, not detected (<0.01%).

contains abundant aluminosilicate and other substances, which can be used as an alternative product of OPC,^{12–17} and this measure can effectively solve metallurgical waste slag disposal. Therefore, many scholars have explored the synthesis of cementing materials by using metallurgical waste slag.

Zhang et al. synthesized a low-carbon binder by using metakaolin and blast furnace slag (BFS) and solidified waste containing heavy metals.¹⁸ Li et al. pointed out that BFS can be used to replace a part of OPC to form a new cementitious material, which can then be utilized to solidify As-contaminated sludge.¹⁹ However, the application of the above solidification/stabilization technology is limited by its poor ability to solidify heavy metals and the low utilization rate of industrial byproducts. The reason for the low solidification rate of As is that many researchers used only the simple physical wrapping and sedimentation of materials to solidify As but did not focus on the As solidification system. Thus, the problem of low solidification efficiency of heavy metals is generated. Considering this problem, some scholars have found that the synthesis of ettringite (AFt) can improve the solidification effect of heavy metals. Hence, several scholars started to synthesize AFt through various means.

The effective activation of aluminosilicate and calcium in industrial byproducts can trigger the formation of AFt and calcium sulfoaluminate monohydrate (AFm), which improve the ability of cementitious materials to solidify As.¹⁸ Cabrera-Luna et al. used CaO as an activator to produce large amounts of AFt and calcium silicate hydrate (C–S–H) from cementitious materials.²⁰ Chen et al. achieved a good solidification effect of heavy metals by adding CaO to form AFt and C–S–H in a fly ash-based polymer.²¹ Li et al. proved the good solidification effect of AFt on As.^{22,23} Some scholars also pointed out the promoting effect of Cl[−] on AFt. Cl[−] can react with AFm calcium trialuminate (C₃A) or Ca(OH)₂ to form small amounts of AFt and C₃A·CaCl₂·10H₂O (Friedel's salt).²⁴ Hou et al. pointed out that the addition of CaCl could promote hydration to generate Cl-AFt, and the test proved that Cl-AFt shows a good solidification effect of As.²⁵ However, most studies only verified the synthesis of AFt through a variety of methods or focused on the solidification of other heavy metals. Studies on the As solidification system of AFt are still lacking. Therefore, we innovatively proposed to stimulate the mass generation of AFt, Fe(Cl)-AFt, and other hydration products through the synergistic effect of CaO and NaCl to improve the solidification efficiency of As and enrich the theory of gel solidification of As. This proposal is important in reducing carbon emissions and resource utilization.

Using the synthesized BFS-based cementitious material (BCM), this study proposes to improve the As solidification efficiency and long-term stability by using the activation mode of CaO and NaCl. First, the effects of CaO and NaCl on the performance of the BCM were studied. Second, the mechanism of As solidification by the BCM gel through the synergistic effect of CaO and NaCl was discussed. Third, the long-term stability of the BCM under the action of CaO and NaCl was determined by performing a leaching toxicity test

and a modified BCR test, and the possible solidification mechanism of As was elucidated. This study introduces a new idea for the low-carbon comprehensive utilization of industrial byproducts, enriches the As solidification mechanism of cementitious materials, and provides a new idea for future research on As solidification.

2. MATERIALS AND METHODS

2.1. Reagents and Materials. The As-containing sludge used in this study comes from a smelter in southern China. Red mud (RM) comes from the alumina plant in southern China. BFS comes from a smelter in southern China. The raw materials, such as BFS, RM, and As-containing sludge, were dried at 65 °C, and the dried material was crushed to 200 mesh with a <20% sieve margin. The phase structure and composition of the raw materials were analyzed by X-ray diffraction (XRD) and X-ray fluorescence (XRF) spectroscopy, as shown in Table 1. The main components of RM are Al₂O₃, CaO, SiO₂, and Na₂O and accompanied by some impurities. Meanwhile, the main components of BFS are CaO, SiO₂, and Al₂O₃. The aforementioned raw materials provide a basis for the collaborative preparation of low-carbon cementitious materials. Figure S1a,b (Supporting Information) shows that BFS and RM are mainly composed of an amorphous phase. BFS is mainly composed of amorphous silicon aluminum glass and some quartz. The main minerals of RM are hydrated calcium zeolite, nepheline, calcite, illite, hydrated sodium aluminosilicate, hematite, sodium titanium oxide, and so forth. These amorphous phases produce a large number of hydration products under alkali activation, thereby improving the mechanical properties and stability of the BCM.²⁶

The XRD and XRF spectra of As-containing sludge are shown in Figure S2 and Table S1. The sodium silicate solution consisted of 7.91% Na₂O, 23.72% SiO₂, and 66.0% H₂O. The alkali activator was synthesized from sodium hydroxide and water glass solution in a certain proportion. The other reagents required for the experiment were of analytical grade.

2.2. Experimental Procedures. The crushed samples were mixed proportionally and stirred for a certain time. The prepared activator was added to deionized water and then to the stirred mixture sample. The experimental scheme is shown in Table 2. After adding the liquid, the mixed sample was placed in a JJ-5 mechanical mixer and stirred for 3 min and then transferred to a cubic mold of 20 mm for solidification. The solidified matrix was cured for 3, 7, and 28 days and kept in 95% relative humidity at a temperature of 20 ± 2 °C and a relative humidity of 95%.²⁷

2.3. UCS and Leaching Tests. The test method for unconfined compressive strength (UCS) was the same as the Test Methods for Wall Bricks.²⁸ A TYE-300F rigid hydraulic pressure servo machine (Jianyi, Wuxi, China) was used to test the UCS of samples cured for 3, 7, and 28 days, respectively. The machine test condition was 2400 N/s.

The China Standard Leaching Test (CSLT) was used as the test method for toxicity leaching.²⁹ The samples to be tested were crushed to <9.5 mm and dried at 60 °C. The method of

Table 2. Mixing Proportions of the Sample and Activator

ID	binder ^a (%)	activator ^b (%)	CaO (%)	As-containing sludge (%)
A0-C0-As0	100	0	0	0
A6-C0-As0	100	6	0	0
A8-C0-As0	100	8	0	0
A10-C0-As0	100	10	0	0
A12-C0-As0	100	12	0	0
A10-C0-As3	100	10	0	3
A10-C4-As3	100	10	4	3
A10-C6-As3	100	10	6	3
A10-C8-As3	100	10	8	3
A10-C10-As3	100	10	10	3
A10-C12-As3	100	10	12	3

^aThe binder is composed of BFS and RM with a mass ratio of 80:20.

^bThe content of this activator is evaluated by the mass of sodium silicate to the binder.

preparing and operating the CSLT is given in the [Supporting Information](#).

2.4. Analysis. The XRD patterns of samples were obtained on an X-ray diffractometer instrument (UltimaIV). The scanning range was 10 to 80° (2θ) with a rate of 10° min⁻¹. Scanning electron microscopy (SEM) was used to observe the microscopic morphology of the sample (TESCAN MIRA LMS). The model of the Fourier transform infrared (FTIR) spectroscopy system used was Thermo IN10, and the test conditions were the same as those for the KBr pellet method. The model of FTIR spectrometer was Zetium.³⁰

3. RESULTS AND DISCUSSION

3.1. Mechanical Properties of the BCM. **3.1.1. Effects of RM on the UCS of the Binder.** [Figure 1](#) shows the change in

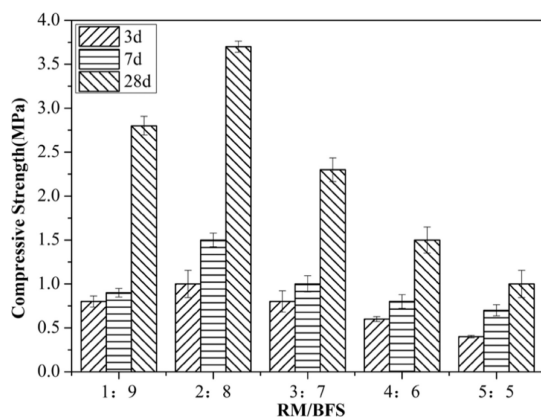


Figure 1. UCS with varying RM contents.

the adhesive UCS after adding different proportions of RM. After 28 days of solidification, the UCS of the binder first increases with increasing RM content and then decreases. The binder with an RM content of 20% has the best UCS. The comparison of the data in [Table 1](#) and [Figure S1](#) shows that RM has a large amount of alkaline components. The increase in RM content increases the alkalinity of the solidified matrix and the UCS and enhances the hydration reaction rate.³¹ However, the UCS of the binder decreases when the added amount of RM exceeds 20% because BFS contains a higher silicoaluminate composition. The hydration products decrease when the silicoaluminate composition decreases, and the

strength declines. Accordingly, the adhesive UCS gradually decreases when the RM content exceeds 20%. Thus, the adhesive with 20% RM is considered to be the best mixture.

We found that the addition of RM will improve the alkalinity of the system, which is conducive not only to the dissolution of aluminosilicate but also to the polymerization reaction, as shown in [Figure 1](#).³² In addition, calcium ions react with dissolved aluminosilicates to form complex hydration products.³³ Therefore, an appropriate increase in alkalinity is the best way to improve the hydration products of adhesives [such as Fe (Cl)-Aft and C-S-H].³⁴

3.1.2. Effect of the Alkali Activator on UCS. The hydration reaction of slag is the pozzolanic reaction between SiO₂, Al₂O₃, and Ca(OH)₂. The addition of an alkali activator has dual functions: (1) it provides a highly alkaline environment for RM and BFS, accelerates the dissolution rate of the calcium- and silicon-rich phases in the phase separation structure of the slag glass phase, and promotes the dissolution of active silicon and aluminum and (2) it provides a large amount of active [SiO₄]⁴⁻ for the slag hydration system, is the main source of the C-S-H gel for hydration products, and increases the reaction rate.³⁵ The regulation mechanism of slag activity excited by an alkali activator is described by [formulas 1–6](#)

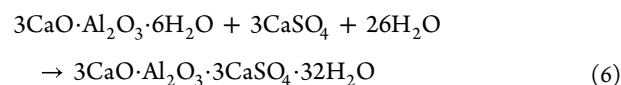
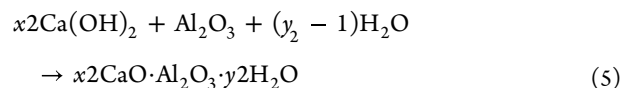
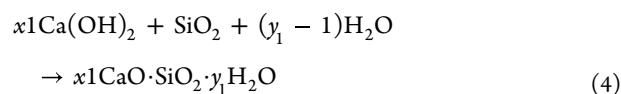
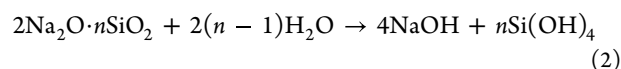


[Figure S3](#) shows the UCS of the BCM with different sodium silicate solution moduli under the condition of added 10% sodium silicate solution. Water glass solutions with different moduli are used as activators of the BCM. Sodium silicate solution increases the alkalinity of the system and accelerates the dissolution of RM and BFS. The formation rate of C-S-H and the geopolymer increases with an increase in the amount of the soluble aluminosilicate component. In addition, sodium silicate solution provides a large amount of silicate and promotes the synthesis of hydration products to enhance the hydration efficiency.³⁵ Hence, the addition of sodium silicate solution can effectively improve the UCS of the BCM. We found that the UCS of the BCM was the highest when the modulus of the water glass solution was 1.0. Meanwhile, the UCS of the BCM decreases when the amount of sodium silicate solution exceeds 10%.^{36,37} This result is consistent with our previous research. A considerable amount of silicate will lead to BCM cracking when the ratio of Si/Al and Si/Ca exceeds the formation conditions of the geopolymer and C-S-H.³⁸ Therefore, the UCS of the BCM is the best when the modulus of the water glass solution is 1.0, and the dosage is

10%. Subsequently, the synthesized BCM was used to solidify As-containing sludge.

3.1.3. Effect of CaO and NaCl on the Solidified Matrix. After the As solidification test of the BCM prepared by the above process, the compressive strength of the BCM significantly decreases when the content of the As-containing waste residue is 3% because the addition of the As-containing waste residue affects the normal progress of the hydration reaction, and the excessive production of new As-containing compounds reduces the compressive strength of the BCM (see Supporting Information, Table S2, for additional data).²³ Although the leaching toxicity of heavy metals significantly decreased, it still did not fall below the standard limit. To improve the As solidification effect and strength of cementitious materials, CaO and NaCl were added to further promote the formation of AFt and realize high-efficiency As solidification. The strengthened BCM (A10-C10-As3) shows a great improvement in the overall UCS under solidification conditions compared with the adhesive (A10-C0-As3) with no added CaO and NaCl, as shown in Figure 2. The addition of

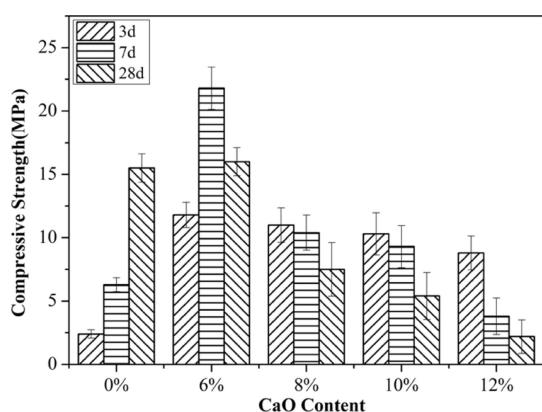


Figure 2. UCS with varying CaO contents.

CaO provides an alkaline environment for the synthesis of hydration products and further improves the hydration efficiency.³⁵ The addition of CaO and NaCl can also improve the production efficiency of AFt, AFm, and Fe (Cl)-AFt compounds.³⁹ The formation of Fe (Cl)-AFt and C-S-H improved the early UCS of the binder. Furthermore, the above-mentioned compounds improve the solidification efficiency of As.⁴⁰ However, the increase in excessive CaO leads to swelling and cracking of the later solidified matrix. The UCS of the binder gradually decreases with increasing CaO content.^{41,42} In addition, the added amount of CaO and NaCl is too small to form enough hydration products such as AFt. Therefore, the binder containing 10% CaO and 1% NaCl is selected as the best matrix.

3.2. Leaching Test. High compressive strength is conducive to the solidification of As. A high compressive strength indicates that the cementitious material obtains As retention through physical encapsulation by forming hydration products and filling pores.^{42,43} In addition, the silicon aluminum structure in slag can form a large number of C-S-H structures under the hydration reaction. These structures improve the immobilization of As by increasing the density and adsorption properties of the BCM.^{44,45} Table 3 shows the leaching concentration of As under different solidification conditions determined by the CSLT method. The As leaching

Table 3. As Concentrations in the CSLT Leachates and CSLT Limits (\leq Means under the Detection Limit)

	3d (mg/L)	7d (mg/L)	28d (mg/L)	CSLT limits (mg/L)
As sludge	480.75			5
A0-C0-As0	0.834	0.77	0.572	
A10-C0-As0	≤ 0.010	≤ 0.010	≤ 0.010	
A10-C0-As3	174.0	105.9	56.88	
A10-C10-As3	0.715	0.453	0.309	

concentration in As sludge (480.75 mg/L) is higher than the CSLT limit (5 mg/L). This finding shows that untreated samples are seriously harmful to the ecological environment. The leaching concentration of As in A10-C8-As3, A10-C10-As3, and A10-C12-As3 is much lower than that in the alkali activator (A10-C0-As3), indicating that the synthesized AFt, Fe (Cl)-AFt, and C-S-H can effectively reduce the leaching concentration of As. We found that the As leaching concentration of A10-C10-As3 containing CaO and NaCl significantly decreased compared with the As leaching concentration of A10-C0-As3. We hypothesize that CaO and NaCl can effectively increase the formation of AFt, Fe (Cl)-AFt, and AFm compared with sodium silicate based on the XRD, FTIR, and SEM analyses.³⁹ The aforementioned results indicate that CaO and NaCl play an important role in the synthesis of AFt, Fe (Cl)-AFt, and AFm. CaO and NaCl were shown to be important in solidifying As in the BCM. The As leaching concentration with CaO and NaCl (A10-C10-As3) and without CaO and NaCl (A10-C0-As3) significantly decreased (from 189.4 to 0.453 mg/L). The leaching results show that the synthesized BCM achieves the purpose of high-efficiency solidification of As, and the solidification rate of As is more than 99.9%.

3.3. Cementitious Mechanisms of the BCM. **3.3.1. XRD Analysis.** The XRD patterns of A0-C0-As0 (a), A10-C0-As0 (b), A10-C0-As3 (c), and A10-C10-As3 (d) are shown in Figure 3. As shown in Figure 3a, the amorphous phase belonging to slag can be observed in the generated composite phase when BFS and RM are combined in a ratio of 80:20, and the characteristic peaks belonging to C-S-H, quartz,

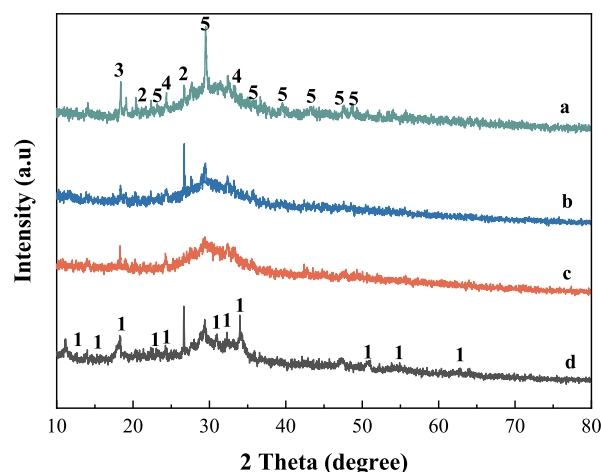


Figure 3. XRD diagrams of A0-C0-As0 (a), A10-C0-As0 (b), A10-C0-As3 (c), and A10-C10-As3 (d). 1, $3\text{CaO}\cdot\text{Al}_2\text{O}_3\cdot 3\text{CaSO}_4\cdot 32\text{H}_2\text{O}$ (PDF# 72-0646); 2, SiO_2 (82-1561); 3, Fe_3O_4 (72-2303); 4, Fe_2O_3 (73-2234); 5, CaCO_3 (88-1812).

magnetite, and hematite can be detected. When a 10% alkali activator is added to activate it on the above basis, it can promote the transformation of the crystalline phase of some substances in the sample, the characteristic peak of hydrated calcium silicate in the composite phase gradually weakens, and some amorphous AFt peaks appear, indicating that the addition of sodium silicate results in the fracture of its chemical bond and the dissolution of silicon ions. The strong alkalinity promotes the dissolution of aluminosilicate.⁴⁶ This result means that the addition of the alkali activator promotes the formation of AFt, and Fe-AFt and AFm compounds are formed under the action of iron ions.⁴⁷ Calcium reacts to form calcium hydroxide under the action of sodium silicate solution.^{48,49} A portion of the produced calcium hydroxide reacts with the dissolved aluminosilicate to form AFt.⁵⁰

The SiO₂ peak in Figure 3c is reduced compared with that in Figure 3b. This result indicates that the addition of As-containing sludge improves the dissolution of aluminosilicate because As-containing sludge has a large amount of gypsum, which can promote the formation of AFt. In addition, the CaSO₄·2H₂O peak gradually decreased, while the AFt peak slowly increased.⁴² When CaO and NaCl are added on the basis of this material, a large amount of AFt can be detected in the crystal phase, as seen in Figure 3d. The addition of CaO and NaCl provides conditions for the formation of AFt, thus promoting the crystal growth of AFt, Fe (Cl)-AFt, and AFm. The increased AFt, Fe (Cl)-AFt, and AFm production can aid in the formation of network structure skeleton support systems, the filling of slurry holes, and the improvement of slurry structure compactness.

An arsenite peak was found in the XRD analysis results in Figure 3d. We speculate that As is mainly solidified in the form of AFt in the BCM. Previous research results show that arsenite has a high As solidification rate and good stability.⁴² These results also prove that the new BCM can effectively improve the solidification speed and stability of As.

3.3.2. FTIR Spectroscopy Analysis. The infrared spectra of A0-C0-As0 (a), A10-C0-As0 (b), A10-C0-As3 (c), and A10-C10-As3 (d) are shown in Figure 4. The characteristic peaks at 472 cm⁻¹ belong to the asymmetric vibration of Al–O and O–Si–O.⁵¹ Meanwhile, the characteristic peaks at 997 and 1433 cm⁻¹ belong to the asymmetric vibration of Si–O–Si and O–C–O,⁵² respectively. The position and intensity of the three

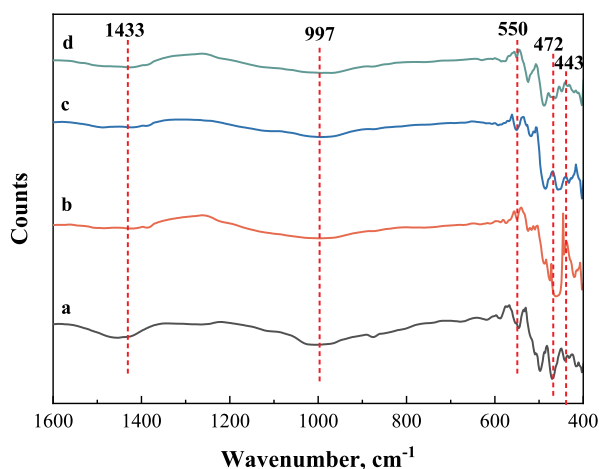


Figure 4. FTIR patterns of A0-C0-As0 (a), A10-C0-As0 (b), A10-C0-As3 (c), and A10-C10-As3 (d).

characteristic peaks changed in various sizes when BFS, RM, and As-containing sludge were compounded in different proportions. Figure 4a shows that the calcite and quartz phases can be detected in the characteristic peak when BFS and RM are compounded in the ratio of 80:20. Furthermore, the characteristic peak from 402 to 550 cm⁻¹ belongs to the bending vibration of Si–O–T (T = Si, Al, Fe) and Fe–O,⁵² indicating the presence of quartz and hematite in the composite phase, which is consistent with the XRD results. We hypothesize that the hydration reaction of BFS and RM can produce C–S–H, which is conducive to improving the mechanical properties, based on previous research results and XRD analysis.⁵³ The infrared characteristics of general C–S–H are Si–O–Si at 455–463 cm⁻¹,⁵² which plays an important role in the strength of cementitious materials.⁵⁴ In Figure 4b, the characteristic peak intensity of calcite, quartz, and hematite in the new material is reduced when the quantitative sodium silicate is added to the composite phase. The addition of sodium silicate destroys the chemical bond in the phase, resulting in the dissolution of Si and Fe ions from the lattice and participating in the network structure of the composite phase. When As-containing sludge, CaO, NaCl, and other substances are continuously added, the intensity and position of the characteristic peak in the range of 443 to 550 cm⁻¹ slightly change,⁵² which is caused by the chemical reaction of Si, Al, and C compounds in the composite phase to form AFt. The addition of CaO provides sufficient Ca²⁺ for the reaction, increases the content of AFt in the composite phase, and provides sufficient active sites for subsequent As solidification. The FTIR results are consistent with the XRD analysis and UCS results. Yu et al. confirmed that CaO can increase the production of AFt.³⁹ The existence of AFt can also improve the stability of the solidified matrix and the efficiency of As solidification.^{23,55} We hypothesize that CaO has a catalytic effect on the synthesis of AFt, Fe (Cl)-AFt, and AFm in the BCM based on the XRD and SEM results. The characteristic band changed with the addition of As sludge.⁵⁶ Therefore, As reacts with Fe (Cl)-AFt and C–S–H to form AFt and other compounds. These results show that CaO and the activator can improve the synthesis efficiency of AFt and Fe (Cl)-AFt in the BCM to further optimize the solidification efficiency of As.⁵⁷

3.3.3. Scanning Electron Microscopy. As seen in Figure 5b, we found a large number of slag particles similar to those in Figure 5a. A small number of columnar structures can be observed in Figure 5b. In comparison with Figure 5b, the sheet structure in Figure 5c sharply increases after an activator is added, increasing the density of the BCM. The addition of CaO and NaCl promotes the formation of AFt, Fe (Cl)-AFt, and AFm and the production of a large number of needle-like structures in Figure 5d compared with those in Figure 5c. These results are consistent with the XRD (Figure 3) and FTIR (Figure 4) results. Specifically, CaO and NaCl can effectively improve the yield of AFt, Fe (Cl)-AFt, and AFm. The newly formed acicular particles fill the pores and increase the density of the BCM.⁵⁸ Therefore, the UCS of the BCM gradually increases.

In combination with our previous studies, we hypothesize that arsenate ions change the structure of AFt. Accordingly, the needle sample in Figure 5d is AFt formed after As solidification. The XRD, FTIR, and SEM results show that CaO and NaCl can improve the formation rate of AFt. The newly formed AFt improves the UCS of the BCM and the

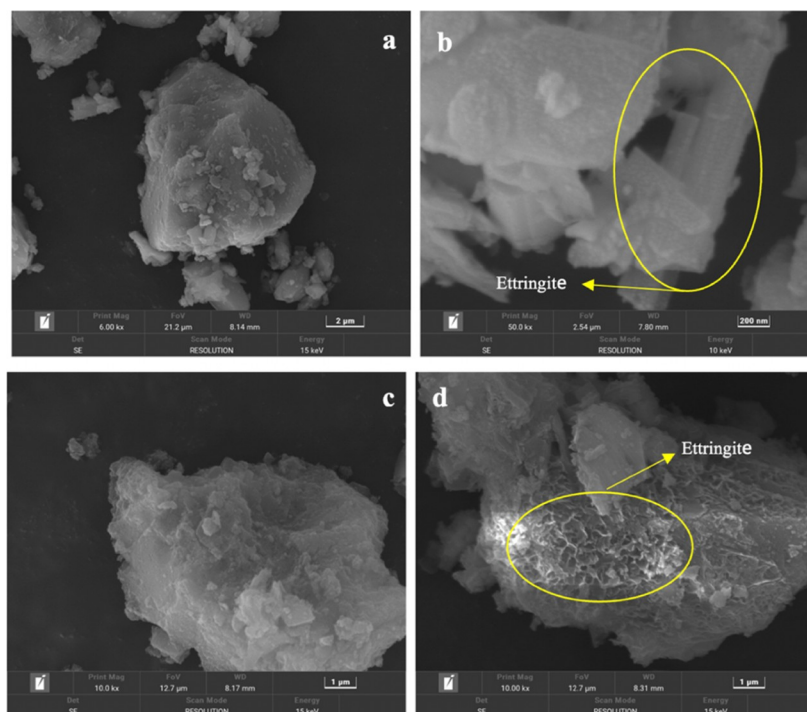


Figure 5. SEM images of BFS (a), A0-C0-As0 (b), A10-C0-As0 (c), and A10-C10-As3 (d).

solidification rate and long-term stability of As. Consequently, the new materials we developed have high efficiency and stable As solidification ability. The change rules of the BCM hydration product microstructure and hydration product type under different conditions were analyzed by SEM and energy spectral analysis [SEM–energy-dispersive X-ray spectroscopy (EDS)]. The results are shown in Figure S4 and Table S3. The SEM–EDS analysis results show that the precipitated crystals have Na, Si, Al, Fe, and O as the main elements, and the main hydration products of the BCM system are hydrated calcium sulfoaluminate (C–S–A–H) and C–S–H. The EDS spectra show the distribution of different elements in the microstructure of the best mixture (A10-C10-As3) at 28 days of solidification. We found that As overlaps with Si, Na, Ca, and Al, indicating that it is fixed in N–(C)–S–A–H, C–S–A–H, and C–S–H frameworks. MgO will participate in the hydration reaction of the BCM system because a small amount of Mg is present in BFS. In addition, hematite in RM participated in the hydration reaction process and formed an N–S–A–Fe–H hydration product in some samples under the action of an activator.⁵⁷ The microstructural uniformity and compactness of the hydration product are high, which further explain the reason for the high mechanical strength of the sample.

3.3.4. Speciation Analysis on Heavy Metals. The chemical forms of heavy metals in the BCM were studied using an improved BCR method to explore the long-term stability and safety of the BCM.⁵⁹ Figure S5 shows the chemical forms of some heavy metals in the BCM. The BCR operation steps and data are shown in Supporting Information, Table S4. In the improved BCR test, the proportions of residual and oxidizable states of arsenic increased by 19.6 and 13.5%, respectively, and the stability of heavy metals improved. The chemical form transformation shows that the hydration products formed after the addition of CaO and NaCl play an important role in the solidification process of heavy metals.⁶⁰

Combined with the previous microstructure analysis, As can complex with the hydration products [mainly $\text{Ca}(\text{OH})_2$] of the BCM to form stable Ca–As precipitates, adsorb onto C–S–H gels, or substitute SO_4^{2-} within Aft lattices. However, As also has a higher solubility in the alkaline pore solution ($\text{pH} > 12.5$) of the gelling system. Thus, the content of hydration products would affect the overall As leachability. This illustrates that both the hydration reaction and physical containment jointly determined the strength and leaching properties of the S/S sludge. Therefore, we think that the BCM is safe as a substitute for cement composites.

3.3.5. Ecological Assessment Index. Based on the risk assessment index method, RAC_i represents the risk assessment value of heavy metal i and $\text{RAC}_{i, \text{exchangeable state}} + \text{RAC}_{i, \text{carbonate-bound state}}$ represents the percentage of exchangeable and carbonate-bound states. The sum of the two is the percentage of F1 in BCR in the total amount of corresponding metals. When $\text{F1} < 1\%$, it means that the risk level of the solid waste is zero; when $1\% < \text{F1} < 10\%$, it means there is a low-level risk; when $11\% < \text{F1} < 30\%$, it means there is an intermediate risk; when $31\% < \text{F1} < 50\%$, it means that there is a high risk; and when $\text{F1} > 50\%$, it means that there is a serious environmental risk.

$$\text{RAC}_{i,j} = \frac{C_{i,j}}{C_0} \quad (7)$$

$$\text{RAC}_i = \text{RAC}_{i, \text{exchangeable state}} + \text{RAC}_{i, \text{carbonate-bound state}}$$

where $C_{i,j}$ represents the measured value of the occurrence form of i metal j , mg/kg; C_0 refers to the measured total content of i metal, mg/kg; RAC_i represents the risk assessment value of heavy metal i ; and $\text{RAC}_{i, \text{exchangeable state}} + \text{RAC}_{i, \text{carbonate-bound state}}$ represents the percentage of the exchangeable state and carbonate-bound state. The sum of the two is the percentage of F1 in BCR in the corresponding total metal.

By calculating and analyzing the data using formula 7, the risk assessment index (RAC) of each solidified body under environmental erosion can be obtained, as shown in Table 4.

Table 4. Risk Assessment Index of Arsenic-Containing Solid Waste under Environmental Erosion

A10-C10-As3 RAC (%)	leaching environment		
	landfill sites	acid rain scene	seawater environment
	6	5	3

For the semidynamic erosion process, the RAC value of the solidified body after leaching in the landfill environment is 6%, the RAC value after leaching in the acid rain environment is 5%, and the RAC value after leaching in the seawater environment is 3%, which is in the range of $1\% < F1 < 10\%$, belonging to the low-level environmental risk state.

4. CONCLUSIONS

This study showed that when the added amount of RM is 20%, the modulus of sodium silicate is 1.0; the added amount is 10%, and the added amount of CaO and NaCl is 10% and 1%, respectively. The BCM has good mechanical properties and As solidification ability. The output of AFm, AFt, and Fe-AFt can be improved, and high-efficiency As solidification can be attained by adding an activator. The addition of CaO further increased the output of AFm, AFt, and Fe (Cl)-AFt and the mechanical strength of the BCM. The maximum UCS of the BCM is 21.8 MPa. As leaching toxicity decreased from 480.75 to 0.309 mg/L, and the As solidification rate was as high as 99.9%. The results of the leaching test and improved BCR extraction test show that the BCM has good long-term stability and safety. The BCM synthesized by BFS and RM solves the environmental problems caused by BFS and RM and realizes the efficient and stable solidification of As. In addition, the synthesized BCM meets the standard of mu10 fly ash bricks and may be a potential building material for future research.

In this study, a new method for increasing the production of AFt, Fe (Cl)-AFt, and AFm in the BCM by using CaO and NaCl was proposed. CaO and NaCl improve the solidification efficiency of As and the UCS of the BCM. Further research is needed to determine how CaO and NaCl increase the production of AFt, Fe (Cl)-AFt, and AFm in the BCM.

■ ASSOCIATED CONTENT

SI Supporting Information

The Supporting Information is available free of charge at <https://pubs.acs.org/doi/10.1021/acsomega.2c04302>.

XRD patterns of red mud and blast furnace slag samples; XRD pattern of arsenic-containing sludge; characteristics of arsenic-containing sludge; effect of the alkali activator on compressive strength of the solidified block; comparison of properties of solidified blocks before and after adding calcium oxide and sodium chloride; SEM analysis results of A10-C10-As3 samples; heavy metal leaching amount using the BCR test; improved BCR extraction steps and results; and specific operation method of the CSLT (PDF)

■ AUTHOR INFORMATION

Corresponding Author

Yuan-cheng Li – College of Agriculture and Biological Sciences, Dali University, Dali, Yunnan 671003, China; Key Laboratory of Ecological Microbial Remediation Technology of Yunnan Higher Education Institutes, Dali University, Dali, Yunnan 671003, China; Faculty of Metallurgical and Energy Engineering, Kunming University of Science and Technology, Kunming, Yunnan 650093, China; Email: LYC_DU@163.com

Authors

Hong Quan – College of Agriculture and Biological Sciences, Dali University, Dali, Yunnan 671003, China; Key Laboratory of Ecological Microbial Remediation Technology of Yunnan Higher Education Institutes, Dali University, Dali, Yunnan 671003, China; orcid.org/0000-0002-8812-5072

Hui-juan Yu – College of Agriculture and Biological Sciences, Dali University, Dali, Yunnan 671003, China; Key Laboratory of Ecological Microbial Remediation Technology of Yunnan Higher Education Institutes, Dali University, Dali, Yunnan 671003, China

Xue Yang – College of Agriculture and Biological Sciences, Dali University, Dali, Yunnan 671003, China; Key Laboratory of Ecological Microbial Remediation Technology of Yunnan Higher Education Institutes, Dali University, Dali, Yunnan 671003, China

Dong-peng Lv – College of Agriculture and Biological Sciences, Dali University, Dali, Yunnan 671003, China; Key Laboratory of Ecological Microbial Remediation Technology of Yunnan Higher Education Institutes, Dali University, Dali, Yunnan 671003, China

Xing Zhu – Faculty of Metallurgical and Energy Engineering, Kunming University of Science and Technology, Kunming, Yunnan 650093, China; orcid.org/0000-0003-0534-1712

Complete contact information is available at: <https://pubs.acs.org/10.1021/acsomega.2c04302>

Author Contributions

H.Q. participated in conceptualization; methodology; writing the original draft; investigations; writing, review, and editing of the manuscript. H.-j.Y. participated in investigations. X.Y. participated in investigation and formal analysis. D.-p.L. participated in data curation. X.Z. participated in formal analysis and investigation. Y.-c.L. participated in project administration, supervision, and funding acquisition.

Notes

The authors declare no competing financial interest.

■ ACKNOWLEDGMENTS

The authors are grateful for the financial support from the Basic Research Project of Yunnan Provincial Science and Technology Department (202001AT070019), the Yunnan Province Postdoctoral Science Foundation (ynbh19029), the Project of Yunnan Province Postdoctoral (ynbh19029), and the Yunnan Province Education Department Scientific Research Fund Project (2022Y889).

REFERENCES

- (1) Lei, J.; Peng, B.; Min, X.; Liang, Y.; You, Y.; Chai, L. Modeling and optimization of lime-based stabilization in high alkaline arsenic-bearing sludges with a central composite design. *J. Environ. Sci. Health, Part A* **2017**, *52*, 449–458.
- (2) Liang, Y.; Min, X.; Chai, L.; Wang, M.; Liyang, W.; Pan, Q.; Okido, M. Stabilization of arsenic sludge with mechanochemically modified zero valent iron. *Chemosphere* **2017**, *168*, 1142–1151.
- (3) Shi, M.-q.; Min, X.-b.; Shen, S.; Chai, L.-y.; Ke, K.; Yan, Y.; Liang, Y.-j. Separation and recovery of copper in Cu–As-bearing copper electrowinning black slime by oxidation acid leaching and sulfide precipitation. *Trans. Nonferrous Met. Soc. China* **2021**, *31*, 1103–1112.
- (4) Min, X.; Xu, Q.; Ke, Y.; Xu, H.; Yao, L.; Wang, J.; Ren, H.; Li, T.; Lin, Z. Transformation behavior of the morphology, structure and toxicity of amorphous As₂S₃ during hydrothermal process. *Hydrometallurgy* **2021**, *200*, 105549.
- (5) Min, X.; Li, Y.; Ke, Y.; Shi, M.; Chai, L.; Xue, K. Fe-FeS₂ adsorbent prepared with iron powder and pyrite by facile ball milling and its application for arsenic removal. *Water Sci. Technol.* **2017**, *76*, 192–200.
- (6) Jiang, G.; Min, X.; Ke, Y.; Liang, Y.; Yan, X.; Xu, W.; Lin, Z. Solidification/stabilization of highly toxic arsenic-alkali residue by MSWI fly ash-based cementitious material containing Friedel's salt: Efficiency and mechanism. *J. Hazard. Mater.* **2022**, *425*, 127992.
- (7) He, D.; Luo, Z.; Zeng, X.; Chen, Q.; Zhao, Z.; Cao, W.; Shu, J.; Chen, M. Electrolytic manganese residue disposal based on basic burning raw material: Heavy metals solidification/stabilization and long-term stability. *Sci. Total Environ.* **2022**, *825*, 153774.
- (8) Zhou, X.; Zhang, Z.-f.; Yang, H.; Bao, C.-j.; Wang, J.-s.; Sun, Y.-h.; Liu, D.-w.; Shen, P.-l.; Su, C. Red mud-metakaolin based cementitious material for remediation of arsenic pollution: Stabilization mechanism and leaching behavior of arsenic in lollingite. *J. Environ. Manage.* **2021**, *300*, 113715.
- (9) Maraghechi, H.; Salwocki, S.; Rajabipour, F. Utilisation of alkali activated glass powder in binary mixtures with Portland cement, slag, fly ash and hydrated lime. *Mater. Struct.* **2017**, *50*, 16.
- (10) Benhelal, E.; Shamsaei, E.; Rashid, M. I. Challenges against CO₂ abatement strategies in cement industry: A review. *J. Environ. Sci.* **2021**, *104*, 84–101.
- (11) Jia, Z.; Lin, B. How to achieve the first step of the carbon-neutrality 2060 target in China: The coal substitution perspective. *Energy* **2021**, *233*, 121179.
- (12) Ren, Q.; Zhang, Y.; Long, Y.; Zou, Z.; Pei, J. Crystallisation behaviour of blast furnace slag modified by adding fly ash. *Ceram. Int.* **2018**, *44*, 11628–11634.
- (13) Cheng, R.-j.; Zhang, H.; Li, Y.; Fang, Q.; Wang, B.; Ni, H.-w. Effect of process parameters on dry centrifugal granulation of molten slag by a rotary disk atomizer. *J. Iron Steel Res. Int.* **2021**, *28*, 263–271.
- (14) Piatak, N. M.; Parsons, M. B.; Seal, R. R., II Characteristics and environmental aspects of slag: A review. *Appl. Geochem.* **2015**, *57*, 236–266.
- (15) Li, Y.; Liu, Y.; Gong, X.; Nie, Z.; Cui, S.; Wang, Z.; Chen, W. Environmental impact analysis of blast furnace slag applied to ordinary Portland cement production. *J. Clean. Prod.* **2016**, *120*, 221–230.
- (16) He, J.; Jie, Y.; Zhang, J.; Yu, Y.; Zhang, G. Synthesis and characterization of red mud and rice husk ash-based geopolymer composites. *Cem. Concr. Compos.* **2013**, *37*, 108–118.
- (17) Cho, D.-W.; Yoon, K.; Ahn, Y.; Sun, Y.; Tsang, D. C.; Hou, D.; Ok, Y. S.; Song, H. Fabrication and environmental applications of multifunctional mixed metal-biochar composites (MMBC) from red mud and lignin wastes. *J. Hazard. Mater.* **2019**, *374*, 412–419.
- (18) Zhang, S.; Zhao, Y.; Guo, Z.; Ding, H. Stabilization/solidification of hexavalent chromium containing tailings using low-carbon binders for cemented paste backfill. *J. Environ. Chem. Eng.* **2021**, *9*, 104738.
- (19) Li, J.-s.; Chen, L.; Zhan, B.; Wang, L.; Poon, C. S.; Tsang, D. C. Sustainable stabilization/solidification of arsenic-containing soil by blast slag and cement blends. *Chemosphere* **2021**, *271*, 129868.
- (20) Cabrera-Luna, K.; Maldonado-Bandala, E.; Nieves-Mendoza, D.; Castro-Borges, P.; Perez-Cortes, P.; Escalante García, J. E. Supersulfated cements based on pumice with quicklime, anhydrite and hemihydrate: Characterization and environmental impact. *Cem. Concr. Compos.* **2021**, *124*, 104236.
- (21) Chen, X.; Zhang, J.; Lu, M.; Chen, B.; Gao, S.; Bai, J.; Zhang, H.; Yang, Y. Study on the effect of calcium and sulfur content on the properties of fly ash based geopolymer. *Constr. Build. Mater.* **2022**, *314*, 125650.
- (22) Li, Y.-C.; Min, X.-B.; Chai, L.-Y.; Shi, M.-Q.; Tang, C.-J.; Wang, Q.-W.; Liang, Y.-j.; Lei, J.; Liyang, W.-J. Co-treatment of gypsum sludge and Pb/Zn smelting slag for the solidification of sludge containing arsenic and heavy metals. *J. Environ. Manage.* **2016**, *181*, 756–761.
- (23) Li, Y.-C.; Min, X.-B.; Ke, Y.; Chai, L.-Y.; Shi, M.-Q.; Tang, C.-J.; Wang, Q.-W.; Liang, Y.-j.; Lei, J.; Liu, D.-G. Utilization of red mud and Pb/Zn smelter waste for the synthesis of a red mud-based cementitious material. *J. Hazard. Mater.* **2018**, *344*, 343–349.
- (24) Du, J.; Liu, Z.; Sun, J.; Li, G.; Wu, X.; Li, G.; Lv, Y.; Wang, K. Enhancing concrete sulfate resistance by adding NaCl. *Constr. Build. Mater.* **2022**, *322*, 126370.
- (25) Hou, D.; Li, T.; Han, Q.; Zhang, J. Insight on the sodium and chloride ions adsorption mechanism on the ettringite crystal: Structure, dynamics and interfacial interaction. *Comput. Mater. Sci.* **2018**, *153*, 479–492.
- (26) Sun, B.; Sun, Y.; Ye, G.; De Schutter, G. A mix design methodology of slag and fly ash-based alkali-activated paste. *Cem. Concr. Compos.* **2022**, *126*, 104368.
- (27) Bayraktar, O. Y. Possibilities of disposing silica fume and waste glass powder, which are environmental wastes, by using as a substitute for Portland cement. *Environ. Sci. Pollut. Res.* **2021**, *28*, 16843–16854.
- (28) GB/T2542-2012, *Test Methods for Wall Bricks*; Standardization Administration of China: China, 2012.
- (29) GB5085.3-2007; *Identification Standard of Hazardous Waste—Identification of Leaching Toxicity*: China, 2007.
- (30) Ke, Y.; Peng, N.; Xue, K.; Min, X.; Chai, L.; Pan, Q.; Liang, Y.; Xiao, R.; Wang, Y.; Tang, C.; Liu, H. Sulfidation behavior and mechanism of zinc silicate roasted with pyrite. *Appl. Surf. Sci.* **2018**, *435*, 1011–1019.
- (31) Li, Y.; Min, X.; Ke, Y.; Liu, D.; Tang, C. Preparation of red mud-based geopolymer materials from MSWI fly ash and red mud by mechanical activation. *Waste Manag.* **2019**, *83*, 202–208.
- (32) Tzanakos, K.; Mimilidou, A.; Anastasiadou, K.; Stratakis, A.; Gidaracos, E. Solidification/stabilization of ash from medical waste incineration into geopolymers. *Waste Manag.* **2014**, *34*, 1823–1828.
- (33) Bakharev, T.; Sanjayan, J. G.; Cheng, Y.-B. Resistance of alkali-activated slag concrete to acid attack. *Cem. Concr. Res.* **2003**, *33*, 1607–1611.
- (34) Ren, P.; Ling, T.-C. Roles of chlorine and sulphate in MSWIFA in GGBFS binder: Hydration, mechanical properties and stabilization considerations. *Environ. Pollut.* **2021**, *284*, 117175.
- (35) Rowles, M.; O'Connor, B. Chemical optimisation of the compressive strength of aluminosilicate geopolymers synthesised by sodium silicate activation of metakaolinite. *J. Mater. Chem.* **2003**, *13*, 1161–1165.
- (36) Kaya, K.; Soyer-Uzun, S. Evolution of structural characteristics and compressive strength in red mud–metakaolin based geopolymer systems. *Ceram. Int.* **2016**, *42*, 7406–7413.
- (37) Zhang, M.; El-Korchi, T.; Zhang, G.; Liang, J.; Tao, M. Synthesis factors affecting mechanical properties, microstructure, and chemical composition of red mud–fly ash based geopolymers. *Fuel* **2014**, *134*, 315–325.
- (38) Cuesta, A.; Santacruz, I.; De la Torre, G.; Dapiaggi, M.; Zea-García, J. D.; Aranda, M. A. Local structure and Ca/Si ratio in CSH gels from hydration of blends of tricalcium silicate and silica fume. *Cem. Concr. Res.* **2021**, *143*, 106405.

- (39) Yu, J.; Qian, J.; Tang, J.; Ji, Z.; Fan, Y. Effect of ettringite seed crystals on the properties of calcium sulphoaluminate cement. *Constr. Build. Mater.* **2019**, *207*, 249–257.
- (40) Tolonen, E.-T.; Hu, T.; Rämö, J.; Lassi, U. The removal of sulphate from mine water by precipitation as ettringite and the utilisation of the precipitate as a sorbent for arsenate removal. *J. Environ. Manage.* **2016**, *181*, 856–862.
- (41) Li, Q.; Xu, H.; Li, F.; Li, P.; Shen, L.; Zhai, J. Synthesis of geopolymer composites from blends of CFBC fly and bottom ashes. *Fuel* **2012**, *97*, 366–372.
- (42) Li, Y.; Min, X.; Ke, Y.; Fei, J.; Liu, D.; Tang, C. Immobilization potential and immobilization mechanism of arsenic in cemented paste backfill. *Miner. Eng.* **2019**, *138*, 101–107.
- (43) Doudart de la Grée, G. C. H.; Yu, Q. L.; Brouwers, H. J. H. Assessing the effect of CaSO₄ content on the hydration kinetics, microstructure and mechanical properties of cements containing sugars. *Constr. Build. Mater.* **2017**, *143*, 48–60.
- (44) Coussy, S.; Paktunc, D.; Rose, J.; Benzaazoua, M. Arsenic speciation in cemented paste backfills and synthetic calcium–silicate–hydrates. *Miner. Eng.* **2012**, *39*, 51–61.
- (45) Malviya, R.; Chaudhary, R. Factors affecting hazardous waste solidification/stabilization: A review. *J. Hazard. Mater.* **2006**, *137*, 267–276.
- (46) Phair, J.; Van Deventer, J. Effect of the silicate activator pH on the microstructural characteristics of waste-based geopolymers. *Int. J. Miner. Process.* **2002**, *66*, 121–143.
- (47) Hertel, T.; Van den Bulck, A.; Onisei, S.; Sivakumar, P. P.; Pontikes, Y. Boosting the use of bauxite residue (red mud) in cement-Production of an Fe-rich calciumsulfoaluminate-ferrite clinker and characterisation of the hydration. *Cem. Concr. Res.* **2021**, *145*, 106463.
- (48) Zheng, L.; Wang, C.; Wang, W.; Shi, Y.; Gao, X. Immobilization of MSWI fly ash through geopolymerization: effects of water-wash. *Waste Manag.* **2011**, *31*, 311–317.
- (49) Chen, K.; Lin, W.-T.; Liu, W. Microstructures and mechanical properties of sodium-silicate-activated slag/co-fired fly ash cementless composites. *J. Clean. Prod.* **2020**, *277*, 124025.
- (50) Feng, H.; Li, C.; Shan, H. In-situ synthesis and catalytic activity of ZSM-5 zeolite. *Appl. Clay Sci.* **2009**, *42*, 439–445.
- (51) Sharma, S. K.; Sharma, G.; Sharma, A.; Bhardwaj, K.; Preeti, K.; Singh, K.; Kumar, A.; Pal, V. K.; Choi, E. H.; Singh, S. P.; Kaushik, N. K. Synthesis of silica and carbon-based nanomaterials from rice husk ash by ambient fiery and furnace sweltering using a chemical method. *Appl. Surf. Sci. Adv.* **2022**, *8*, 100225.
- (52) Kapeluszna, E.; Kotwica, Ł.; Rózycka, A.; Gołek, Ł. Incorporation of Al in CASH gels with various Ca/Si and Al/Si ratio: Microstructural and structural characteristics with DTA/TG, XRD, FTIR and TEM analysis. *Constr. Build. Mater.* **2017**, *155*, 643–653.
- (53) Palomo, A.; Grutzeck, M. W.; Blanco, M. T. Alkali-activated fly ashes: A cement for the future. *Cem. Concr. Res.* **1999**, *29*, 1323–1329.
- (54) Shilin, C., *Effect of Ferric Chloride on Microstructure of Hydrated Calcium Silicate and Ettringite*; Journal of Shijiazhuang Tiedao University (Natural Science Edition), 2020; Vol. 33, p 4.
- (55) Zhang, D.; Wang, S.; Wang, Y.; Gomez, M. A.; Jia, Y. The long-term stability of calcium arsenates: Implications for phase transformation and arsenic mobilization. *J. Environ. Sci.* **2019**, *84*, 29–41.
- (56) Yan, M.; Huang, Y.; He, H.; Xie, Y.; Li, Y. Efficient removal of arsenic (III) from aqueous solutions by new layered hydroxides (Ca–Fe–Cl LDHs). *J. Dispersion Sci. Technol.* **2021**, *42*, 998–1008.
- (57) Yu, L.; Mengyuan, L.; Peiyu, Y. Effect of Mineral Admixtures on Rheological Properties and Thixotropy of Binder Paste. *J. Chin. Ceram. Soc.* **2019**, *47*, 594–601.
- (58) Lin, K.; Lin, D. Hydration characteristics of municipal solid waste incinerator bottom ash slag as a pozzolanic material for use in cement. *Cem. Concr. Compos.* **2006**, *28*, 817–823.
- (59) Wen, J.; Yi, Y.; Zeng, G. Effects of modified zeolite on the removal and stabilization of heavy metals in contaminated lake sediment using BCR sequential extraction. *J. Environ. Manage.* **2016**, *178*, 63–69.
- (60) Li, E.; Yang, T.; Wang, Q.; Yu, Z.; Tian, S.; Wang, X. Long-term stability of arsenic calcium residue (ACR) treated with FeSO₄ and H₂SO₄: Function of H⁺ and Fe (II). *J. Hazard. Mater.* **2021**, *420*, 126549.